

# International Journal of Pharmaceutics

## Development of samarium doped phosphate glass microspheres for internal radiotherapy applications

--Manuscript Draft--

<b>Manuscript Number:</b>	IJPHARM-D-23-03505R1
<b>Article Type:</b>	Research Paper
<b>Section/Category:</b>	Personalised Medicine
<b>Keywords:</b>	flame spheroidisation; internal radiotherapy; microspheres; samarium-doped phosphate glass
<b>Corresponding Author:</b>	Ifty Ahmed University of Nottingham UNITED KINGDOM
<b>First Author:</b>	Andi Arjuna
<b>Order of Authors:</b>	Andi Arjuna
	Ben Milborne
	Amal Reska Putra
	Theresia Rina Mulyaningsih
	Herlan Setiawan
	Md Towhidul Islam
	Reda Felfel
	Ifty Ahmed
<b>Abstract:</b>	<p>Delivering radioactive sources within the body, into cancerous tissues can be particularly effective to reduce tumour size, especially when external beam radiotherapy is not possible. A pure beta emitter, <math>^{90}\text{Y}</math> is currently used for internal radiotherapy. However, theranostic radionuclide-doped microspheres can be developed by incorporating <math>^{153}\text{Sm}</math> that emits both therapeutic beta and diagnostic gamma energies. This study investigated the production of high concentrations of samarium content doped phosphate-based glass microspheres. The glass P60 (i.e. <math>60\text{P}_2\text{O}_5\text{-}25\text{CaO-}15\text{Na}_2\text{O}</math>) was mixed with <math>\text{Sm}_2\text{O}_3</math> at ratios of 75:25 (G75:Sm25), 50:50 (G50:Sm50) and 25:75 (G25:Sm75) and processed via flame spheroidisation. SEM and EDX confirmed the microsphere uniformity with significantly high samarium content up to 44% in G25:Sm75. Via XRD analysis, samarium-doped microspheres appeared to be a glass-ceramic in nature. Mass-loss, size and pH changes were performed over 28 days, revealed a significant increase in samarium microspheres stability. After 15 minutes neutron activation (neutron flux <math>3.01 \times 10^{13} \text{ n.cm}^{-2}.\text{s}^{-1}</math>) the specific activity of the microspheres (G75:Sm25, G50:Sm50 and G25:Sm75) was 0.28, 0.54 and 0.58 GBq.g<sup>-1</sup>, respectively. Therefore, this study confirms that developed samarium microspheres provide a great potential for improving the internal radiotherapy for cancers, by avoiding complex procedures, using less microspheres and shortening irradiation time.</p>
<b>Suggested Reviewers:</b>	Eneko Larraneta, Dr Senior Lecturer, Queen's University Belfast e.larraneta@qub.ac.uk
	Andi Dian Permana, Dr Professor, Hasanuddin University andi.dian.permana@farmasi.unhas.ac.id
	Jamieson Christie, Dr Senior Lecturer, Loughborough University j.k.christie@lboro.ac.uk
	Richard Martin, Dr





The University of  
Nottingham

UNITED KINGDOM • CHINA • MALAYSIA

Faculty of Engineering  
University Park Campus  
Nottingham  
NG7 2RD  
t: 01157484675

e: [ifty.ahmed@nottingham.ac.uk](mailto:ifty.ahmed@nottingham.ac.uk)

<https://www.nottingham.ac.uk/engineering/people/ifty.ahmed>

31st Oct 2023

**The Editor**

International Journal of Pharmaceutics

**Reference:** Developing Samarium-doped Phosphate Glass Microspheres for Internal Radiotherapy Applications

Dear Editor

We hereby submit our manuscript entitled “Developing Samarium-doped Phosphate Glass Microspheres for Internal Radiotherapy Applications” for publication consideration in the “International Journal of Pharmaceutics”. We also confirm that this manuscript has not been previously published (in any language) and not submitted for publication elsewhere. Furthermore, the authors have no conflicts of interest.

This study summarises a new approach to producing samarium microspheres via a single stage flame spheroidisation process developed in our group. This is then followed by nuclear activation of the microspheres to transform non-radioactive  $^{152}\text{Sm}$  into  $^{153}\text{Sm}$  for potential internal radiotherapy applications to treat liver and bone cancers (locally). The study also shows how the theranostic characteristics enabled by  $^{153}\text{Sm}$  are hugely advantageous over current commercially available pure beta emitter microspheres.

The microspheres produced have been analysed using SEM to confirm their morphology, EDX analysis to verify composition, XRD and FTIR-ATR to understand their structure, degradation study to confirm microsphere stability and Neutron Activation Analysis (NAA) alongside Gamma spectroscopy to determine their radioactivity. The microspheres produced had uniform morphology with significantly high samarium content achieved (approximately 44% for G25:Sm75). These samarium containing microspheres formed a glass-ceramic structure and were highly stable with increasing samarium content. Importantly, with only 15 minutes of irradiation, the specific radioactivity of  $^{153}\text{Sm}$  reached 0.58 GBq/g, which estimates to approximately 3 – 6 times higher than the yttrium-containing microspheres currently on the market (i.e., Therasphere).

This study highlights that the samarium microspheres developed provide great potential for improving current internal radiotherapy cancer treatments by using less microspheres, reduced irradiation time and increased microsphere stability. Importantly, these samarium microspheres are both beta emitters (for therapeutic) and gamma emitters (for diagnostic) which will avoid the need of complex pre and post treatment currently required for pure beta emitter radionuclide doped microspheres.



We would very much appreciate the opportunity for review and consideration for publication in your journal and look forward to hearing from you in due course. Many thanks in advance.

Yours sincerely



Dr Ifty Ahmed

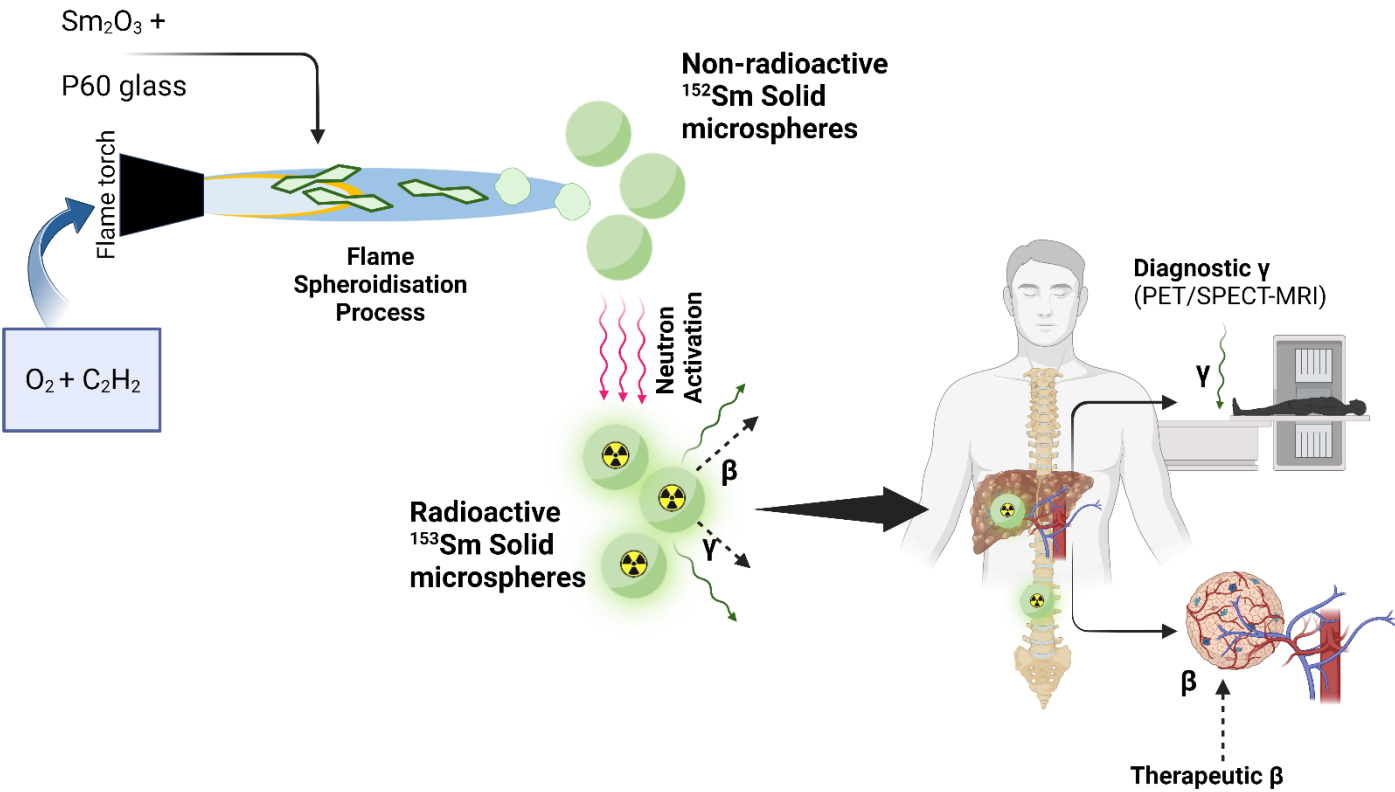
Associate Professor

Advanced Materials Research Group

# Graphical Abstract

## Development of samarium-doped phosphate glass microspheres for internal radiotherapy applications

Andi Arjuna, Ben Milborne, Amal Reska Putra, Theresia Rina Mulyaningsih, Herlan Setiawan, Md Towhidul Islam, Reda Felfel, Ifty Ahmed



**Declaration of interests**

☒The authors declare that they have no known competing financial interests or personal relationships that could have appeared to influence the work reported in this paper.

☐The authors declare the following financial interests/personal relationships which may be considered as potential competing interests:

**Author Contributions:**

A.A.: Investigation, formal analysis, visualisation, drafting original manuscript, writing review and editing

B.M.: Investigation;

A.RP.: Investigation;

T.RM: Resources and Methodology;

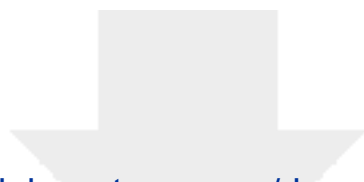
H.S.: Resources and Methodology;

M.TI.: Investigation;

R.F.: Conceptualisation and supervision;

I.A.: Conceptualisation, methodology, supervision and writing—review and editing.

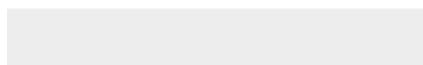
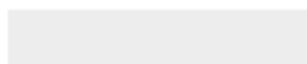
All authors have read and agreed to the published version of the manuscript.



[Click here to access/download](#)

**Supplementary Material**

ESI Manuscript IP\_Andi ARJUNA 011123.docx





# Development of samarium-doped phosphate glass microspheres for internal radiotheranostic applications

Andi Arjuna<sup>1,2</sup>, Ben Milborne<sup>1</sup>, Amal Rezka Putra<sup>3</sup>, Theresia Rina Mulyaningsih<sup>3</sup>, Herlan Setiawan<sup>3</sup>, Md Towhidul Islam<sup>1</sup>, Reda Felfel<sup>1</sup>, Ifty Ahmed<sup>1</sup>

<sup>1</sup>*Advanced Materials Research Group, Faculty of Engineering, University of Nottingham, Nottingham NG7 2RD, U.K.*

<sup>2</sup>*Faculty of Pharmacy, Hasanuddin University, Makassar 90245, Indonesia*

<sup>3</sup>*Research Organization for Nuclear Energy (ORTN), National Research and Innovation Agency (BRIN), Tangerang Selatan, Banten 15314, Indonesia*

## \*Corresponding author:

Ifty Ahmed

Advanced Materials Research Group, Faculty of Engineering, University of Nottingham, Nottingham

Email: [ifty.ahmed@nottingham.ac.uk](mailto:ifty.ahmed@nottingham.ac.uk)

## Abstract

Internal radiotherapy delivers radioactive sources inside the body, near to or into malignant tumours, which may be particularly effective when malignancies are not responding to external beam radiotherapy. A pure beta emitter, <sup>90</sup>Y, is currently used for internal radiotherapy. However, theranostic radionuclide-doped microspheres can be developed by incorporating <sup>153</sup>Sm, which emits therapeutic beta and diagnostic gamma energies. This study investigated the production of high concentrations of samarium-content doped phosphate-based glass microspheres. The glass P60 (i.e. 60P<sub>2</sub>O<sub>5</sub>-25CaO-15Na<sub>2</sub>O) was mixed with Sm<sub>2</sub>O<sub>3</sub> at ratios of 75:25 (G75:Sm25), 50:50 (G50:Sm50) and 25:75 (G25:Sm75) and processed via flame spheroidisation. Scanning electron microscopy (SEM) and energy dispersive X-ray (EDX) confirmed the microsphere uniformity with significantly high samarium content up to 44% in G25:Sm75. Via X-ray diffraction (XRD) analysis, samarium-doped microspheres appeared to be glass-ceramic in nature. Mass-loss, size and pH changes were performed over 28 days, revealing a significant increase in samarium microsphere stability. After 15 minutes of neutron activation (neutron flux 3.01 X 10<sup>13</sup> n.cm<sup>-2</sup>.s<sup>-1</sup>), the specific activity of the microspheres (G75:Sm25, G50:Sm50 and G25:Sm75) was 0.28, 0.54 and 0.58 GBq.g<sup>-1</sup>, respectively. Therefore, the samarium microspheres produced in this study provide great potential for improving internal radiotherapy treatment for liver cancer by avoiding complex procedures and using less microspheres with shorter irradiation time.

1  
2  
3  
4  
5  
6  
7  
8  
9  
10  
11  
12  
13  
14  
15  
16  
17  
18  
19  
20  
21  
22  
23  
24  
25  
26  
27  
28  
29  
30  
31  
32  
33  
34  
35   **Keywords:** flame spheroidisation, internal radiotherapy, microspheres, samarium-doped  
36   phosphate glass  
37  
38  
39  
40  
41  
42  
43  
44  
45  
46  
47  
48  
49  
50  
51  
52  
53  
54  
55  
56  
57  
58  
59  
60  
61  
62  
63  
64  
65

## 1. Introduction

In 2020, over 900,000 new cases of liver cancer (Hepatocellular carcinoma - HCC), including both primary and metastatic, were reported, making it the sixth most common cancer to be diagnosed globally (Foglia, Turato, and Cannito 2023; “Liver Cancer Statistics | Cancer Research U.K.” 2022). Surgical resection is usually the primary curative treatment for suitable patients. However, symptoms of liver cancer are sometimes undetectable until the disease has proceeded to intermediate or late stages, where more than 75% of patients were diagnosed when curative treatment was no longer applicable (Bruix et al. 2016; Y. H. Wong et al. 2019; Nurul Ab Aziz Hashikin et al. 2015). As such, therapy has focussed on systemic treatments, external beam radiotherapy and/or palliative treatments.

Transarterial radioembolisation (TARE) is a minimally invasive method of delivering radioembolic microspheres through intra-arterial routes (Meza-Junco et al. 2012). Microspheres with diameters ranging from 20 to 60 microns are delivered through the capillaries of liver tumours to provide a localised radiation dose while preserving healthy tissues (Meza-Junco et al. 2012; Kauffman et al. 2023). TheraSphere™ (Boston Scientific Corporation, Canada) and SIR-Spheres® (SIRTex, Sydney, Australia) are currently used as radioembolic agents for hepatic radioembolisation (Kauffman et al. 2023). After intra-arterial delivery to the targeted tumour, these microspheres operate similarly to brachytherapy implants, delivering therapeutic doses of (beta) radiation in situ. These commercially available microspheres use the same radioisotope, yttrium-90 (<sup>90</sup>Y), as their therapeutic radiation source (Kauffman et al. 2023; Milborne et al. 2020; Weber et al. 2022).

As the radioisotope <sup>90</sup>Y is a pure beta emitter, verifying microsphere distribution in situ via post-procedural imaging has been challenging. The <sup>90</sup>Y bremsstrahlung imaging method may only produce a limited spatial resolution, which can significantly decrease image quality (Tan et al. 2022). In addition, longer acquisition times due to the low true-coincidence counter rate for positron emissions may restrict the quantity accuracy of <sup>90</sup>Y microspheres PET imaging (Pasciak et al. 2014; Kao et al. 2013). Therefore, to assess therapeutic outcomes, a lung shunting study is commonly conducted using macro-aggregated albumin (MAA) labelled with Technetium-99m (<sup>99m</sup>Tc) to evaluate the distribution of the microspheres in the liver and lungs (Y. H. Wong et al. 2019; Tan et al. 2022). Even though the <sup>99m</sup>Tc has been considerably precise for dosimetry purposes, combining therapeutic irradiation therapy with the capacity to provide diagnostic data concurrently at the cancer site would be highly beneficial.

A theranostic radionuclide emitting both therapeutic beta and diagnostic gamma energies would be an advancement over the pure beta emitter microspheres (Sadler et al. 2022). For example, a samarium in the form of  $^{153}\text{Sm}$  can be used for this purpose since it has a physical half-life of 46.3 hours and a thermal neutron activation cross-section of 210 barns. It can emit beta particles with energies of 0.81 MeV (20%), 0.71 MeV (30%), and 0.64 MeV (50%) (Sadler et al. 2022; Nurul Ab Aziz Hashikin et al. 2015), as well as gamma photons with energies of 103 keV (28%) (Sadler et al. 2022; Wong et al. 2019). The production of  $^{153}\text{Sm}$  with appropriate therapeutic action and radionuclide purity via neutron activation has previously been explored (Hashikin et al. 2015; Wong et al. 2019; Yeong et al. 2020; Wong et al. 2020).  $\text{SmCl}_3$  was formulated as microparticles using Amberlite<sup>TM</sup> IR-120 H+ (Hashikin et al. 2015) and Fractogel EMD  $\text{SO}^{3-}$  resins as a base (Hashikin et al. 2015). Negatively charged acrylic microspheres labelled with  $^{153}\text{Sm}$  have also been explored for transarterial hepatic radioembolisation producing samarium-153 loaded resin microspheres (Wong et al. 2019). Furthermore, the use of samarium as a radiation source for other oncology treatments, such as bone cancer, has also been studied.  $^{153}\text{Sm}$  has been used for palliative pain therapy for bone metastases in the form of samarium leixidronam (Anderson and Nunez 2007). Ceramic seeds containing  $^{153}\text{Sm}$  have also been developed by incorporating  $\text{Sm}_2\text{O}_3$  into  $\text{SiO}_2$  and  $\text{CaO}$  using a sol-gel processing method, resulting in a cylindrical-shaped seed 0.75 mm in diameter and 1.6 mm in length (Valente et al. 2011), as an implant to treat bone metastases. Each of these brachytherapy products utilised different samarium-based  $^{152}\text{Sm}$  to be activated into  $^{153}\text{Sm}$  prior to administration. In addition, with the existence of radiovertebroplasty therapy, combining radioactivity with bone cement for treating spinal metastases (Donanzam et al. 2013), finding the optimum matrix that could locally deliver samarium into the tumour area would also be hugely beneficial.

Despite ongoing efforts to use samarium-based brachytherapy products, geometry, size, uniformity, distribution and limited concentration of samarium in the matrices used have thus far limited their development. For example, spherical-shaped products show better uniformity in size and shape as well as greater surface area and flow properties when compared to irregular-shaped particles (Islam et al. 2017; Hossain et al. 2018). Further, achieving higher radionuclide content in the product may also allow for increased radiation to be delivered to the target site via a reduced quantity of materials used and a potential reduction in neutron activation durations (d'Abadie et al. 2021).

Several materials, including resins, polymers, albumins and liposomes, have been investigated as radioisotope delivery systems (Peltek et al. 2019). However, these bases may cause radioisotope leakage and early release, potentially migrating and thus irradiating healthy cells away from the intended tumour site of interest (Knapp and Dash 2016; Sofou 2008). Glasses have very high resistance to radiation and are generally non-toxic (Milborne et al. 2020). Successful use of glasses as radioisotope carrier matrices has been shown in TheraSphere™, based on a silicate glass matrix (Kauffman et al., 2023; Milborne et al., 2020). Some studies (Nijssen et al. 1999; Sharifi et al. 2022) have suggested that glasses are ineffective for in situ radiotherapy due to their density, which may impact their mobility in arteries. However, the density problem could be overcome by controlling the microsphere sizes and structures.

Phosphate-based glasses (PBGs) are unique bioresorbable glasses with great potential for internal radiation delivery due to their tailorable formulations, which control their physical, chemical, bioactivity and dissolution properties to suit the intended application (Islam et al. 2017; Hossain et al. 2018). PBGs also have relatively low melting temperatures, enabling glass preparation and various post-processing techniques to form unique geometries, including microspheres, fibres, discs and microtubes (Ahmed et al. 2019).

This study developed samarium oxide-doped PBG microspheres for potential applications in delivering radiotherapy via hepatic radioembolisation, overcoming the limitations of <sup>90</sup>Y microspheres highlighted above. The manufacture of PBG formulations and processing into microspheres using flame spheroidisation, physicochemical characteristics (SEM, EDX, XRD), stability and radioactivity profiles are also characterised and discussed in this study. Since PBGs as the matrix can be formulated to have a similar composition to the bone, the microspheres produced could also feasibly be employed for radiovertebroplasty therapy.

## **2. Material and methods**

### **2.1 Materials**

The P60 (60P<sub>2</sub>O<sub>5</sub>-25CaO-15Na<sub>2</sub>O) glass was prepared using the following precursors: phosphorus pentoxide (P<sub>2</sub>O<sub>5</sub>) (Fisher Scientific, U.K., ≥99%), sodium dihydrogen phosphate (NaH<sub>2</sub>PO<sub>4</sub>) (Sigma Aldrich, UK, ≥99%), and calcium phosphate dibasic (CaHPO<sub>4</sub>) (Sigma Aldrich, UK, ≥99%). The microspheres were prepared by mixing phosphate-based glass and P60 powder with Sm<sub>2</sub>O<sub>3</sub> prior to flame spheroidisation.

### **2.2 P60 glass preparation**

The P60 glass is composed of P<sub>2</sub>O<sub>5</sub> (60 mol%), CaO (25 mol%) and Na<sub>2</sub>O (15 mol%). The required amounts of precursor powder were weighed accurately and mixed thoroughly together. The mixed powder was then poured into a 100 ml volume Pt/Rh crucible (Birmingham Metal Company, U.K.) and placed into a furnace. The temperature was set in two cycles: 350°C for 30 minutes and 1150°C for 90 minutes. The resulting molten glass was poured onto a steel plate and left to cool to room temperature. The resulting glass was then ground using a ball mill (Retsch PM 100) and sieved to achieve powder particle size ranges of 45-63 µm, 63-125 µm and 125-200 µm.

### 2.3 Microsphere production

The P60 glass powder was processed into microspheres using a flame spheroidisation utilising an MK74 thermal spray gun (Metallisation Ltd, Bham, U.K). The process was operated using a 3:3 ratio of Oxygen:Acetylene gases. To prepare the samarium-containing microspheres, the P60 glass powders were mixed with Sm<sub>2</sub>O<sub>3</sub> powder with different ratios of glass P60:Sm<sub>2</sub>O<sub>3</sub>, as presented in **Table 1**. The respective powders were mixed using a pestle and mortar and then processed via a flame spheroidisation using the same P60 microspheres production setup. The resulting microspheres, both samarium and P60 microspheres as a control, were collected and sieved again (between 63 – 125 µm and 125 – 200 µm) for characterisation.

**Table 1.** Comparison and microspheres formulation code used for preparation and characterisation.

Microspheres code	P60 glass powder ratio (%)	Sm <sub>2</sub> O <sub>3</sub> ratio (%)
P60	100	-
G75:Sm25	75	25
G50:Sm50	50	50
G25:Sm75	25	75

### 2.4 Scanning Electron Microscopy (SEM) analysis

The morphology of all microspheres produced was observed using scanning electron microscopy (SEM) JEOL 6490 LV SEM. The analysis was conducted with an accelerating voltage of 15 kV at a working distance of 10 mm and a spot size of 50. Prior to analysis, respective samples were fixed onto aluminium stubs with conductive carbon tabs and sputter coated with platinum.

### 2.5 Energy Dispersive X-ray (EDX) analysis

The composition of the microspheres was examined through EDX (Oxford Instruments INCA, U.K.) with an accelerating voltage of 15 kV at a working distance of 10 mm and a spot size of 50 – 60. The solid microsphere samples were mounted on double-sided carbon tape and coated with carbon (Quorum coater). The composition analysis was run through map and point analysis on large and small areas at several points (minimum 8) to quantify the amount of P, Na, Ca, O, and Sm present.

## **2.6 X-ray diffraction (XRD) analysis**

X-ray diffraction analysis was used to investigate the resulting structure of the microspheres produced. The nature structure of microspheres was observed using a Bruker D8 Advanced diffractometer (Bruker AXS, Germany), room temperature with Ni-filtered CuK $\alpha$  radiation ( $\lambda=0.15418$  nm), generated at 40 kV and 35 mA. Data were collected from 8° to 50° diffraction angle (2 $\Theta$ ) using a scan step time of 8 s, step size of 0.04° and a 5° glancing angle. Any crystalline peaks detected were identified using the EVA software (DIFFRACplus suite, Bruker-AXS) and the International Centre for Diffraction Data (ICDD) database.

## **2.7 Fourier transform infrared (FTIR) spectroscopy analysis**

Infrared spectroscopy was performed to observe the structural character of microspheres produced using a Bruker Tensor-27 spectrometer (Bruker Optics, Germany). The spectra were run in a wavenumber region of 400 to 4000 cm<sup>-1</sup> in absorbance mode, followed by the analysis conducted through the OPUS software 5.5.

## **2.8 Mass loss, size changes and pH analysis**

Degradation studies of the microspheres produced were conducted based on mass-loss, size change and pH changes of the media over 28 days. Mass-loss measurements were carried out using microspheres in the size range of 125-200  $\mu$ m placed in Milli-Q water as immersion media. Each formulation's mass (400 mg) was measured before and after degradation in Milli-Q water media (40 ml) at 37°C over 28 days. At each respective time point (1, 3, 7, 14, 21 and 28 days), the microspheres were filtered and placed in an oven at 50°C for 24 hours to dry prior to weight measurement.

Further in-depth investigations were also conducted to explore the microsphere size changes over the same period. Here, microspheres were sieved into a narrow size range of 63-71  $\mu$ m (to

significantly reduce a wide starting size distribution) and placed in vials filled with 40 ml of Milli-Q water. At each time point (days 1, 3, 7, 14, 21, and 28), the microspheres were filtered and left to dry in an oven at 50°C for 24 hours. The pH of the media was also measured (using a pH meter Mettler Toledo, Switzerland). The media was refreshed at each point in time, with three replicate analyses conducted in this study. The dry microspheres were then prepared for SEM and EDX analysis (as mentioned in sections 2.4 and 2.5) and the changes in microspheres sizes were measured. The SEM images obtained for measurement were analysed using ImageJ software.

## 2.9 Neutron activation analysis (NAA)

The microspheres produced were also analysed for neutron activation analysis at the Research Centre for Radiation Detection and Nuclear Analysis Technology, National Research and Innovation Agency, Indonesia. The G.A Siwabessy Multipurpose Reactor (GAS-MPR) regularly operated at a 15 M.W. power level. GAS-MPR is an open pond-type research reactor fuelled with Uranium Silicide (U<sub>3</sub>Si<sub>2</sub>-Al) with a 2.96 g/cm<sup>3</sup> density and an average flux of  $2 \times 10^{14}$  n/cm<sup>2</sup>. second. The measurement parameters used are presented in **Table 2**.

**Table 2.** Working parameters used for neutron activation analysis.

Parameters	Notes
Reactor	G.A. Siwabessy Multipurpose Reactor (GAS-MPR)
Thermal Neutron Flux, $\Phi$ (n.cm <sup>-2</sup> .s <sup>-1</sup> )	$3.01 \times 10^{13}$
Sample Loading System	Rabbit System Facility
Sample Container	LDPE vials
Sample Weight (g)	0.026
Irradiation Time (s)	900
Irradiation Location	Peripheral to the core
Sample Delivery	Automatic-hydraulic system
Data Acquisition	Gamma-ray spectrometry
Sample Counting Time	1 – 2 hours

The microparticles were sealed in individual low-density polyethylene (LDPE) wrapped in aluminium foil and placed into polyethylene capsules for irradiation. The targets were irradiated for 15 minutes at 15 M.W. power. After activation, the samples were left for 3-4 days to allow



for complete decay of short-lived contaminant radionuclides that may appear. The radioactivity of the samples was then measured using an HPGe detector from Canberra.

## 2.10 Gamma spectrometry analysis

Gamma spectrometry was conducted using an HPGe detector with Genie 200 software after 3 – 4 days of decay time. The gamma spectra were analysed based on the net areas under the gamma peaks as the total count for each the considered gamma energy where the energy efficiency was calculated according to the following equation:

$$\varepsilon = \frac{N}{\text{Live Time} \times \text{Activity} \times \text{Yield}} \quad \text{Equation 1}$$

where; N = net peak area (counts), Live time = the actual counting time (s), A = activity of the standard source (Bq), and Yield is obtained from the certificate of the authoritative source or library.

## 2.11 Statistical analysis

All data were presented, calculated and processed using GraphPad Prism. Where it is applicable, the data displayed is based on mean  $\pm$  S.D.

## 3. Results

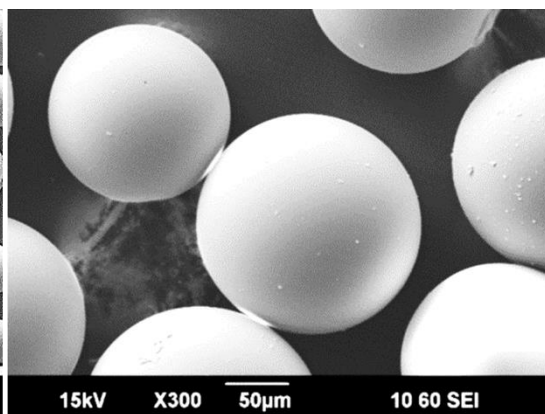
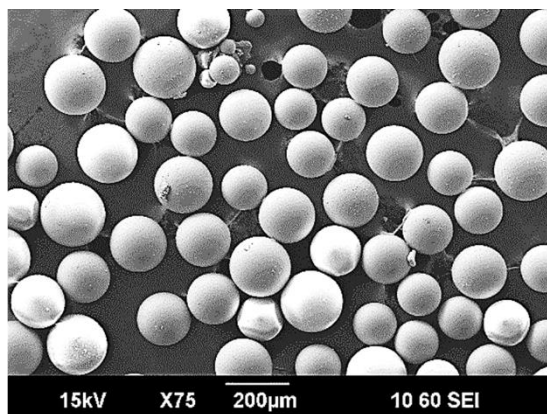
In this study, exploring how much samarium could be incorporated within phosphate-glass matrices was initially conducted. Samarium oxide ( $\text{Sm}_2\text{O}_3$ ) was mixed with phosphate-based glass  $60\text{P}_2\text{O}_5.25\text{CaO}.15\text{Na}_2\text{O}$  (P60) powder at three different ratios for processing into solid (dense) microspheres via a flame spheroidisation methodology developed in our group. The P60: $\text{Sm}_2\text{O}_3$  ratios were 75:25 (G75:Sm25), 50:50 (G50:Sm50), and 25:75 (G25:Sm75). The microspheres produced were separated using sieves into a size range of 125-200  $\mu\text{m}$  for further characterisation. The properties of the three microsphere ratio products were compared to the P60 solid microspheres and  $\text{Sm}_2\text{O}_3$  powder as control groups.

### 3.1 Morphology analysis via Scanning Electron Microscopy (SEM)

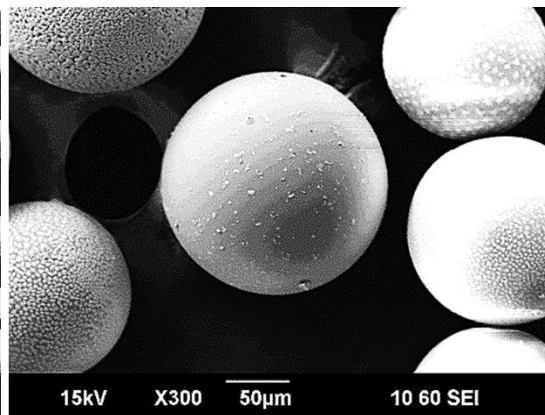
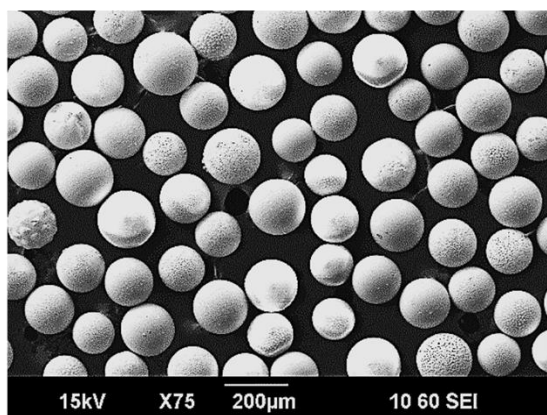
The solid microspheres' morphology is presented in **Figure 1**, which shows that the sieved products were perfectly spherical.

1  
2  
3  
4  
5  
6  
7  
8  
9  
10  
11  
12  
13  
14  
15  
16  
17  
18  
19  
20  
21  
22  
23  
24  
25  
26  
27  
28  
29  
30  
31  
32  
33  
34  
35  
36  
37  
38  
39  
40  
41  
42  
43  
44  
45  
46  
47  
48  
49  
50  
51  
52  
53  
54  
55  
56  
57  
58  
59  
60  
61  
62  
63  
64  
65

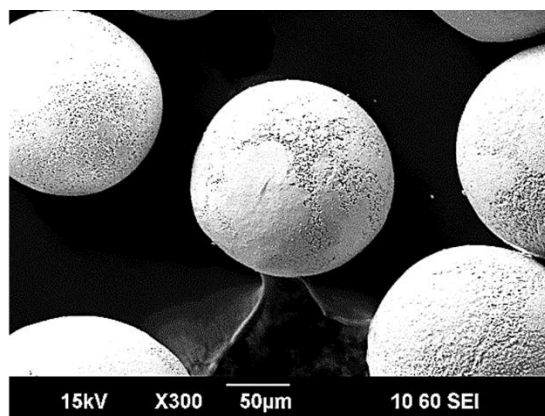
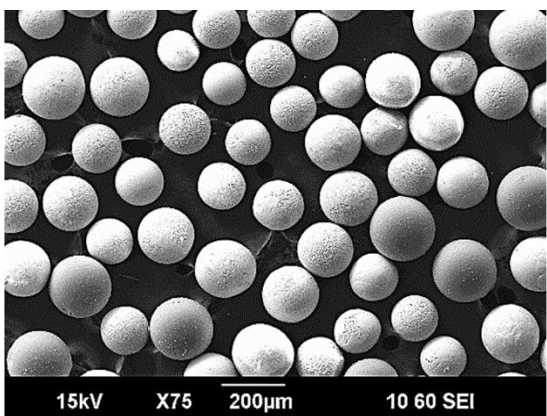
A



B



C



D

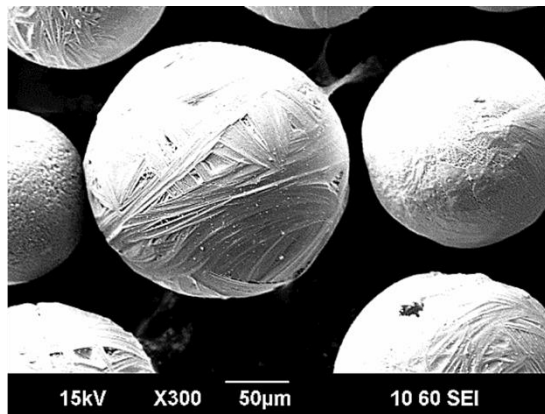
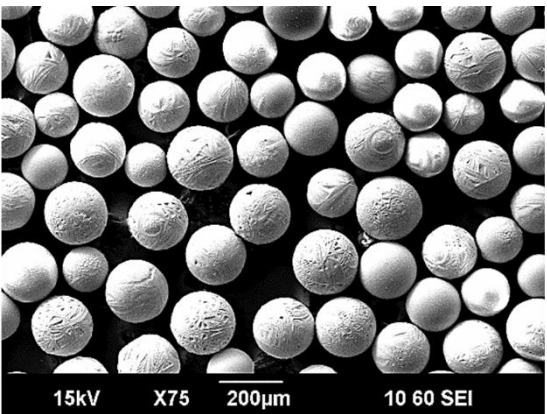


**Figure 1.** SEM images of solid microspheres A) P60, B) G75:Sm25, C) G50:Sm50 and D) G25:Sm75.

### 3.2 Composition via Energy Dispersive X-ray (EDX) Analysis

The compositions of microspheres produced were confirmed via EDX analysis and are shown in **Figure 2**. Samarium oxide was successfully doped into P60 at each ratio investigated. The content of  $\text{Sm}_2\text{O}_3$  in G75:Sm25 was  $14 \pm 2$  mol% with a significant increase to  $33 \pm 3$  mol% and  $44 \pm 5$  mol% in each of G50:Sm50 and G25:Sm75 formulation. All the glass constituents within the microspheres decreased proportionally as the amount of samarium oxide added to the glass increased (see **Figure 2**).

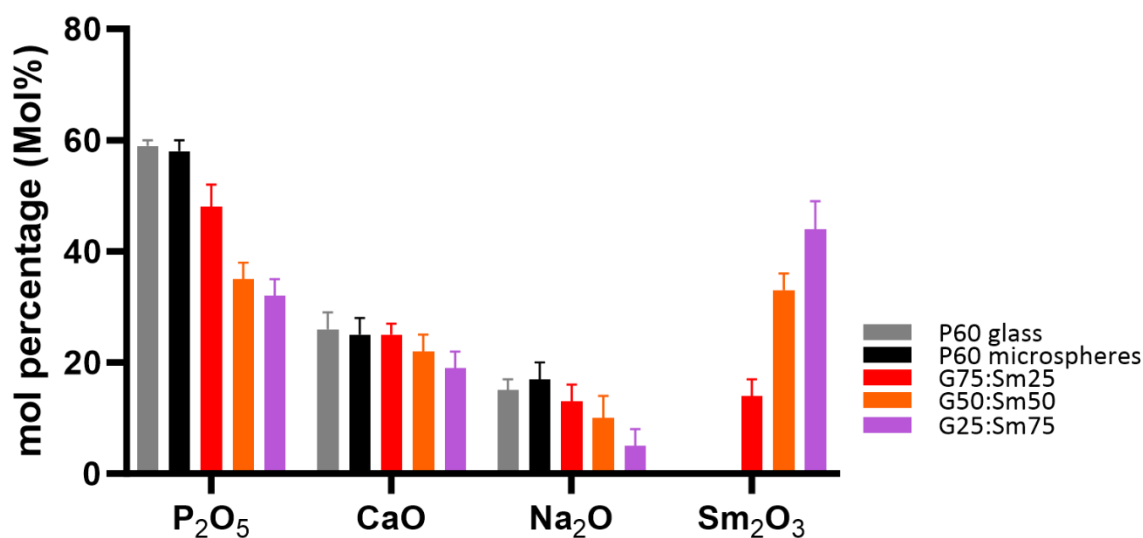


**Figure 2.** The composition of the solid samarium microsphere produced compared to P60 glass alone via EDX.

### 3.3 Structural analysis via X-ray Diffraction (XRD)

The diffraction patterns obtained for the microspheres produced are shown in **Figure 3**. Three broad peaks were seen between  $\sim 20 - 60^\circ$  ( $2\theta$ ) alongside the absence of any detectable sharp crystalline peaks confirming the amorphous nature of the P60 microspheres produced via flame spheroidisation. However, several crystalline peaks were observed in the XRD pattern for the G75:Sm25, G50:Sm50 and G25:Sm75 microsphere samples. For these samarium-containing microspheres, the crystalline phases were identified as samarium oxide (1) ICDD No.00-042-1464 and samarium phosphate (2) ICDD No.00-034-1006 for the three microsphere

formulations whilst retaining the characteristic broad peaks at 20-60° which corresponded to the starting P60 phosphate glass. Sm<sub>2</sub>O<sub>3</sub> was also run as a control.

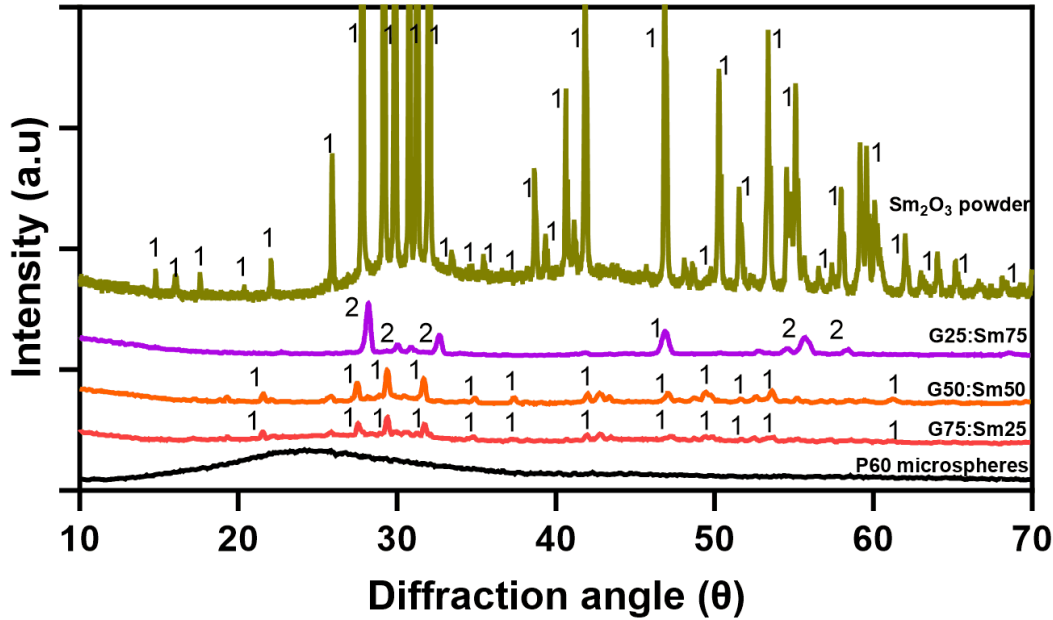


**Figure 3.** X-ray diffraction patterns of solid microspheres and Sm<sub>2</sub>O<sub>3</sub> as a control. The peaks are labelled (1) samarium oxide phase, ICDD No. 00-042-1464, whereas (2) represents samarium phosphate phase, ICDD No. 00-034-1006.

### 3.4 Structural analysis via Fourier Transform Infrared (FTIR) Spectroscopy

**Figure 4** shows the FTIR spectra obtained through Attenuated Total Reflection (ATR) showing the absorbance value, recorded at 500 – 1500 cm<sup>-1</sup>. Solid microspheres P60 exhibited at least two distinctive vibrations: 1) 720-750 and 800-1000 cm<sup>-1</sup>, which were assigned for  $\nu_s(\text{P-O-P})$  and  $\nu_{as}(\text{PO}_2)$  of two bridging oxygens in Q<sup>2</sup> species (Marzouk et al. 2019; Dousti et al. 2013; Arafat, Samad, Wadge, et al. 2020). The band at 2) 900-1300 cm<sup>-1</sup> was assigned for  $\nu_s$  and  $\nu_{as}$  for non-bridging or terminal oxygens in Q<sup>2</sup> species (Marzouk et al. 2019; Dousti et al. 2013; Hussain et al. 2017) [35,36,37]. The appearance of these prominent bands was also observed for the other three microspheres produced: G75:Sm25, G50:Sm50 and G25:Sm75.

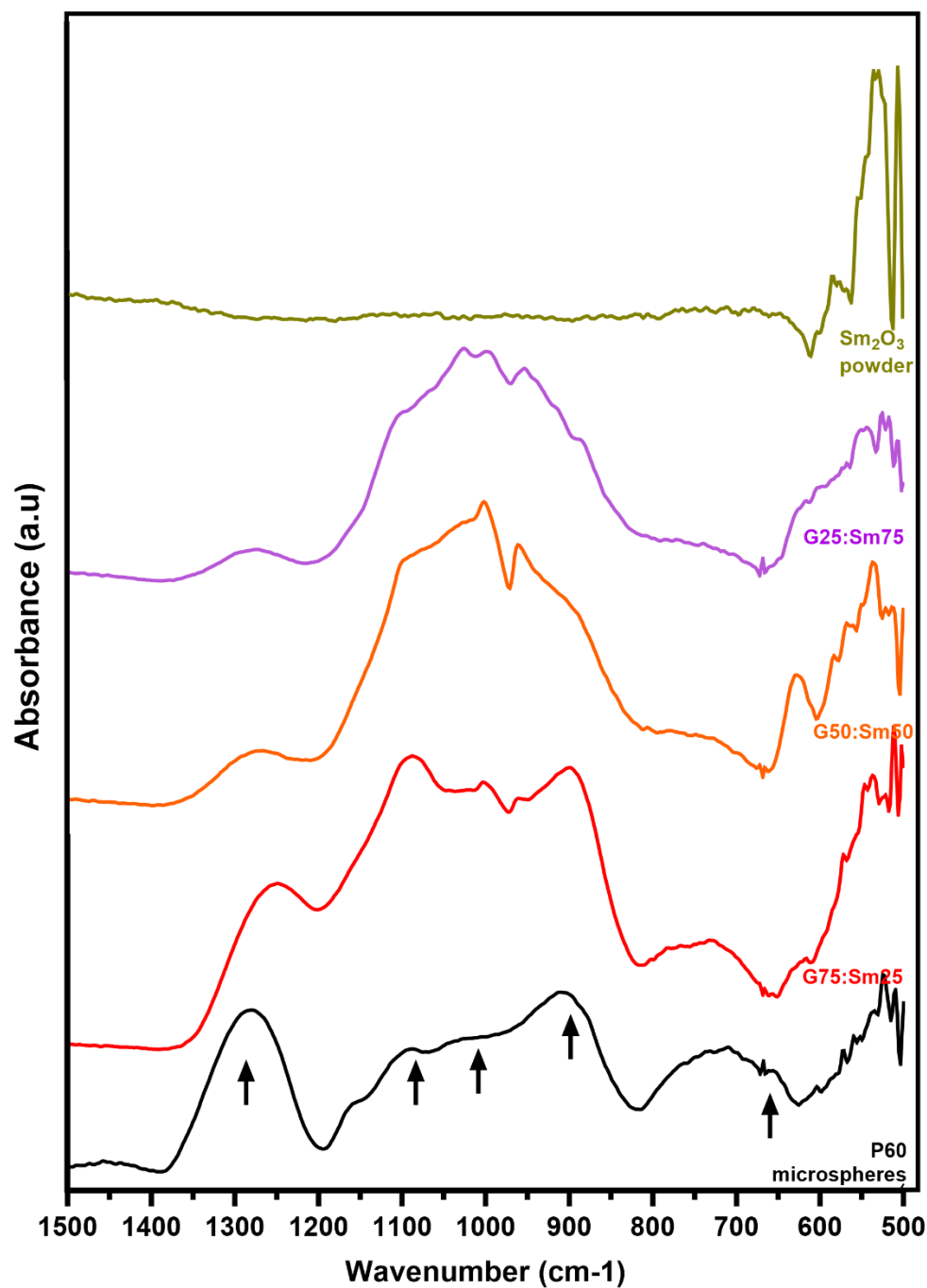
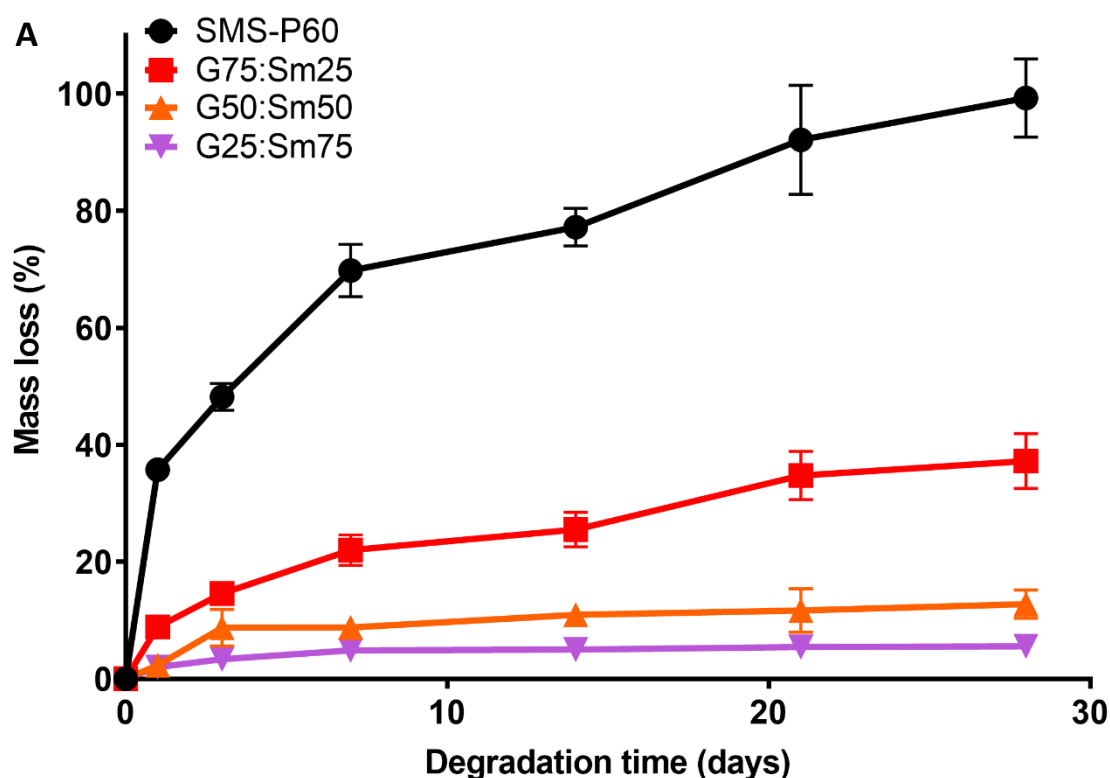


**Figure 4.** FTIR spectra of the samarium-containing microspheres compared to solid P60 microspheres and  $\text{Sm}_2\text{O}_3$  powder as a control. The analysis was run through ATR which recorded the absorbance value.

### 3.5 Degradation study

A degradation study was performed by immersing the microsphere products in Milli-Q water and observing changes over 28 days. Weight changes (mass loss), size and pH of the degradation media were monitored at varying time points over the evaluation period. **Figure**

5.A shows the mass loss percentage of each microsphere's ratios determined at several time points (day 1, 3, 7, 14, 21, and 28) in Milli-Q water. By day 14, the P60 microspheres had degraded extensively, exhibiting an approximate 80% decrease in mass, which continuously increased to 100% by the end of the study (day 28). In contrast, G75:Sm25, G50:Sm50 and G25:Sm75 experienced only slight decreases in mass by day 14. G75:Sm25 showed an approximate 25% decrease in mass by this stage, whereas only a maximum 10% and 8% decrease were observed for G50:Sm50 and G25:Sm75 microspheres, respectively.



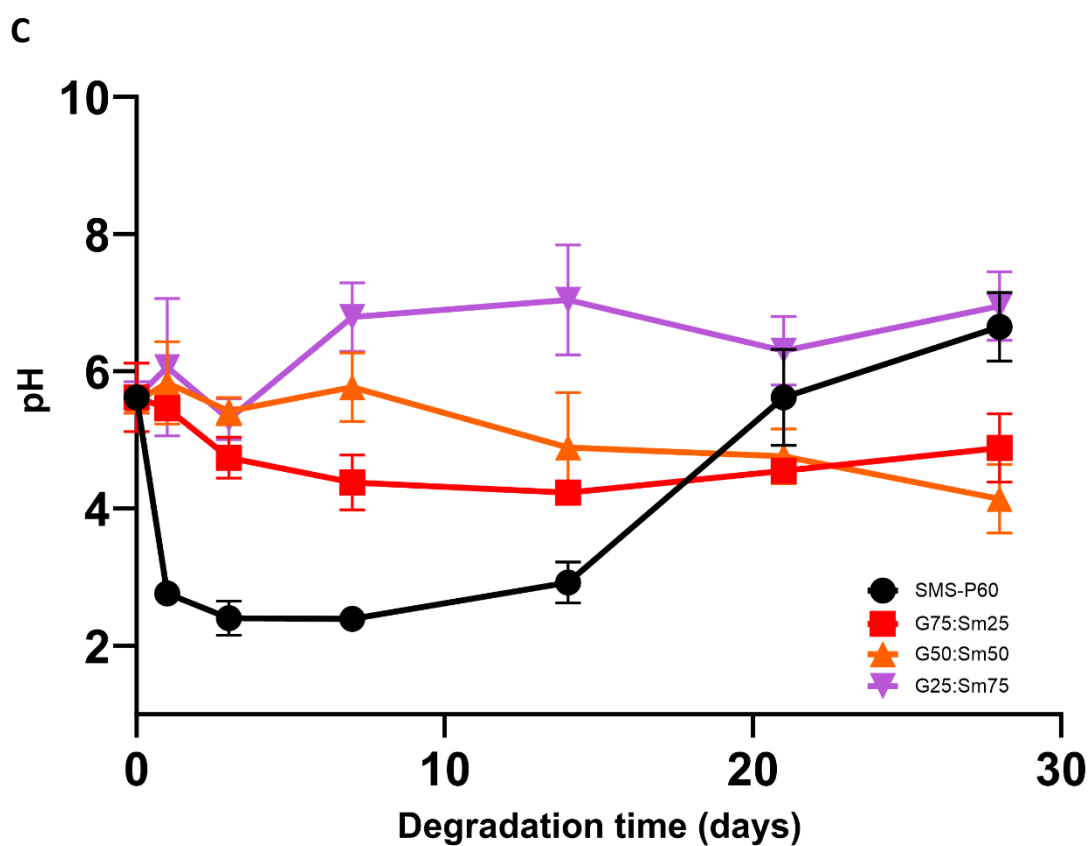
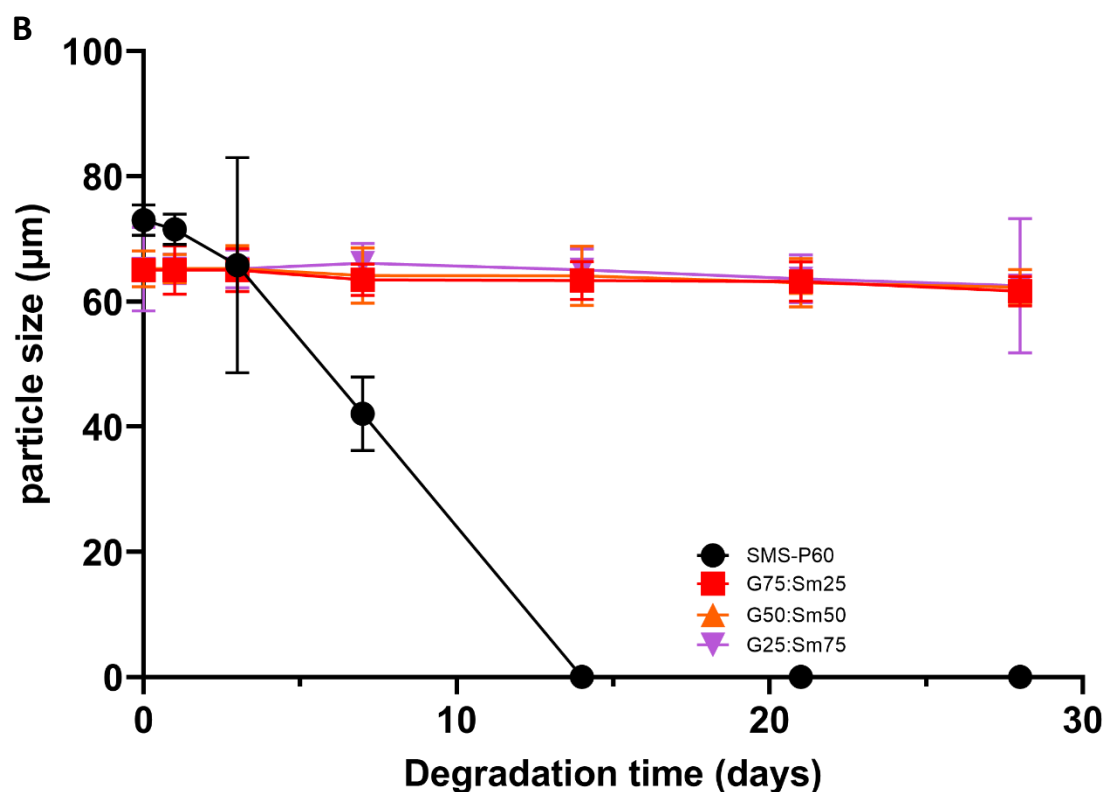


**Figure 5.** (A) Percentage mass loss (B) Size changes of the microspheres as a function of immersion time (day) in Milli-Q water at 37° C over 28 days. (C) pH changes of media Milli-Q water during degradation study over 28 days.

Furthermore, degradation studies of the microspheres were also conducted by observing their change in size over 28 days immersed in Milli-Q water. This study was performed by initially selecting a very narrow particle size range (63 - 71  $\mu\text{m}$ ) of the microspheres to minimise error in data collection. SEM analysis combined with Image J software was employed to measure the size of the microspheres over time. As seen in **Figure 5.B**, the P60 microspheres appeared to experience almost a 100% reduction in particle size by day 14, whereas the other microspheres showed stable size up to day 28.

The change in pH of the Milli-Q water was also observed over the 28 days and presented in **Figure 5.C**. A rapid decrease in pH was seen by day 1 for the P60 microspheres which correlated to the significant mass loss and size reduction observed (see **Figures 5.A** and **5.B**). The media of P60 revealed a rapid decrease to pH of  $2.76 \pm 0.05$  after only one day. Further, after the day-14 time point, the pH increased gradually to 6.65 by day 28, comparable to the fresh solution's starting pH. However, the pH of all solutions with samarium-containing microsphere samples remained relatively stable around the starting pH (6) of the Milli-Q water.

### 3.6 Initial radioactivity analysis of activated microspheres

The initial radioactivity analysis for the samples has been explored via neutron activation analysis and gamma spectroscopy. The analysis was conducted for 15 min irradiation time per sample. As presented in **Table 3**, the neutron-activated  $^{153}\text{Sm}$  in samarium microspheres achieved a maximum specific radioactivity calculated using **Equation 1**, which was at 0.58 GBq/g.

**Table 3.** Radioactivity and gamma spectrometry profile at peak energy  $103.1 \pm 0.2$  keV of samarium-153 in microspheres post-neutron activation

Microspheres	Peak Energy (keV)	Net peak area (net count)	Time decay (seconds)	$A_{t,d}$ (GBq/g)	$A_0$ (GBq/g)
<b>G75:Sm25</b>	103.21	1.15E+006	1219926	0.0017	0.28
<b>G50:Sm50</b>	103.17	2.26E+006	1224234	0.0033	0.54
<b>G25:Sm75</b>	103.2	2.37E+007	1230629	0.0035	0.58

$A_{t,d}$  = Activity was determined after time decay storage

$A_0$  = Activity was determined from  $A_{t,d}$  value,  $t_{1/2}$  and decay constant ( $\lambda$ ) of  $^{153}\text{Sm}$

Furthermore, the radioactivity of activated samarium in the microspheres was also estimated through the neutron activation formula [Eq.1] below:

$$A_t = \sigma_{act} \varphi N (1 - e^{-\lambda t}) \text{ Equation 2}$$



where:

$A_t$  = activity at known irradiation time (Bq),  $\sigma_{act}$  = thermal neutron activation cross-section (barns),  $\phi$  = neutron flux ( $n.cm^{-2}.s^{-1}$ ),  $N$  = number of parent atoms (m/w) x isotopic abundance x  $6.023 \times 10^{23}$ ,  $\lambda$  = decay constant ( $s^{-1}$ ),  $t$  = irradiation time (s).

Utilising the data obtained in **Table 3** and the formula in **Equation 2**, it was determined that 3 hours of irradiation time (see **Table 4**) would be sufficient for the samarium containing samples to achieve more than 3 GBq/g radioactivity (see Table 2).

**Table 4.** Radioactivity estimation of samarium-153 in microspheres using neutron activation equation (Eq 2) for different irradiation times.

Microspheres	$A_t$ (t = 60 min) (GBq/g)	$A_t$ (t = 90 min) (GBq/g)	$A_t$ (t = 3 hours) (GBq/g)
<b>G75:Sm25</b>	1.1	1.64	3.23
<b>G50:Sm50</b>	2.16	3.23	6.39
<b>G25:Sm75</b>	2.31	3.47	6.85

#### 4. Discussion

This study aimed at developing samarium oxide-doped phosphate glass microspheres for potential internal radiotherapy applications in treating liver and/or bone cancers. Currently, yttrium is the only radionuclide-doped microsphere-based glass approved by the FDA for selective internal radiotherapy (SIRT), brachytherapy for liver cancer. The concentration of yttrium incorporated in a silicate glass matrix for this product named ‘TheraSphere’ is ~17 mol% (Kawashita et al. 2011); hence, that level was a minimum benchmark to achieve. Previous studies by Arafat *et al.* (2020) reported that 5 mol% yttrium oxide could be doped into phosphate glass  $45\text{P}_2\text{O}_5-(30-x)\text{Na}_2\text{O}-25\text{CaO}-x\text{Y}_2\text{O}_3$  through a melt-quenching method and that subsequent increases of  $\text{Y}_2\text{O}_3$  content led to the crystallisation of the glass.

Establishing high concentrations of radionuclides would likely have an impact on the efficiency of the radiation dose delivered whilst effectively reducing irradiation time during nuclear activation before administration (Hashikin et al. 2015). Based on the minimum benchmark threshold set, it was realised that adding significantly higher concentrations of a radionuclide (in oxide form) was not possible via the glass melt quench route. Therefore, to incorporate high levels of samarium oxide, the research group further developed the novel flame spheroidisation (F.S.) processing method to increase the samarium oxide content in the microspheres produced.

To achieve high samarium content,  $\text{Sm}_2\text{O}_3$  was mixed with P60 phosphate-based glass ( $60\text{P}_2\text{O}_5.25\text{CaO}.15\text{Na}_2\text{O}$ ) formulation using the following P60: $\text{Sm}_2\text{O}_3$  ratios: 75:25 (G75:Sm25), 50:50 (G50:Sm50) and 25:75 (G25:Sm75), before the F.S. process. The ratios were selected to explore the quantity of samarium that could be effectively incorporated into the phosphate-based glass matrix. The starting P60 and  $\text{Sm}_2\text{O}_3$  powder mixture was comprised of particles with irregular shapes, which were transformed into microspheres with uniform spherical shapes after the F.S. process, as shown in **Figure 1**. The formation of the spherical geometry was regulated by surface tension during the cooling phase when the molten particles were ejected from the flame (Molinar Díaz et al., n.d.; Milborne et al., 2022). The F.S. production process facilitated the adequate melting of  $\text{Sm}_2\text{O}_3$  (melting point  $2,335^\circ\text{C}$ ) (Kaur et al. 2023) when combined with the P60 formulation and subjected to a high-temperature flame ( $\sim 3100^\circ\text{C}$ ) (Molinar Díaz et al., n.d.), which led to the successful production of high samarium-content microspheres.

The formulations of the microspheres produced were confirmed via EDX analysis (see **Figure 2**), where it was found that the  $P_2O_5$  content decreased with increasing concentrations of samarium oxide as expected. The starting  $P_2O_5$  content in the P60 glass powder was  $59 \pm 1$  mol%, with no significant changes having occurred when processed into P60 microspheres at  $58 \pm 2$  mol%. However, this content decreased significantly by 19%, 40% and 46% in each of the G75:Sm25, G50:Sm50 and G25:Sm75, ratio samples produced. In addition, a drastic reduction was also seen in the  $Na_2O$  content from  $17 \pm 3$  mol% in P60 microspheres to  $5 \pm 2$  mol% in G25:Sm75. Overall, the EDX analyses confirmed that the F.S. process could produce microspheres with high concentrations of samarium at 33% mol% (G50:Sm50) and 44 mol% (G25:Sm75), respectively. In addition, the high  $Sm_2O_3$  content was also shown to be evenly distributed (see **Figure S1a**, Supporting Information) whilst maintaining uniformity in its morphology.

Further, XRD analysis initially confirmed the amorphous structure of the phosphate P60 microspheres by the absence of crystalline peaks and the presence of broad (halo) peaks between  $20-40^\circ$ . However, crystalline phases were observed for G75:Sm25 and G50:Sm50 microspheres, which were assigned to samarium oxide (ICDD No. 00-042-1464). Whilst a samarium phosphate (ICDD No. 00-034-1006) phase was observed for the G25:Sm75 microspheres (see **Figure 3**). The appearance of crystalline peaks associated with both samarium oxide and samarium phosphate alongside the presence of a broad halo peak (indicating the presence of an amorphous phase) suggested that the formation of a glass-ceramic material had occurred for all the samarium-containing microspheres. Adding increasing concentrations of  $Sm_2O_3$  (from 25-75 wt%) led to crystallisation of the base P60 glass, which was in line with the study by Lim *et al.* (2021) where samarium-doped  $Y_2Mo_3O_{12}$  ceramic was prepared through a solid-state reaction method. They showed that as the amount of  $Sm^{3+}$  content increased, a transition of phases occurred where new phases of samarium molybdates were formed along with a  $Y_2Mo_3O_{12}$  phase (Lim *et al.* 2021).

The FTIR-ATR analysis (**Figure 4**) performed highlighted that the P60 phosphate glass microspheres consisted of  $Q^2$  and  $Q^3$  network groups (Dousti *et al.*, 2013; Marzouk *et al.*, 2019). The band at  $500-600\text{ cm}^{-1}$  for the P60 microspheres was assigned to the bending of P-O-P (Marzouk *et al.* 2019), which remained present in all the samarium-containing microspheres. The band at  $720-750\text{ cm}^{-1}$  was assigned to symmetric stretching of the P-O-P band (Dousti *et al.* 2013; Marzouk *et al.* 2019; Arafat *et al.* 2020) and the band at  $800-1000$

cm<sup>-1</sup> correlated to asymmetric stretching vibrations of PO<sub>2</sub> groups (Dousti et al. 2013). Hussain *et al.* (2017) studied the optical characteristics of Sm<sup>3+</sup>-doped phosphate glass ((i.e. 60 – x)P<sub>2</sub>O<sub>5</sub>-30ZnO-10MgO-xSm<sub>2</sub>O<sub>3</sub>, where x = 0.1 – 1.0 mol%) and suggested that the asymmetric and symmetric stretching vibrations of P–O–P linkages observed in the FTIR spectra of that glass were characteristic of Q<sup>3</sup> and Q<sup>2</sup> groups which resided due to the conversion of bridging oxygens to non-bridging oxygens. In all samarium-containing microspheres, these bands shifted slightly to higher wavenumbers with increasing Sm<sub>2</sub>O<sub>3</sub> content. Arafat *et al.* (2020) reported that the absorption band at 703 cm<sup>-1</sup> assigned to the P-O-P linkage shifted to a higher wavenumber (around 719 cm<sup>-1</sup>) and a band shift at around 880 cm<sup>-1</sup> to a lower wavenumber with increasing Y<sub>2</sub>O<sub>3</sub> content implied that depolymerisation of the phosphate network had occurred. Furthermore, peaks in the frequency range of 900–1250 cm<sup>-1</sup> were assigned to the symmetric and asymmetric stretching modes of non-bridging or terminal P–O bonds (Dousti et al. 2013; Marzouk et al. 2019; Hussain et al. 2017) for the Q<sup>2</sup> species.

The durability of the resulting microspheres was also investigated by observing for changes in mass loss, particle size and pH of the immersion media. As shown in **Figure 5**, a good correlation was observed between the mass loss, size reduction and pH change of the degradation medium. Starting from day 3, a significant increase in mass loss to 48 ± 2 % was observed for P60 microspheres as a control. Under these conditions, the pH of the media was also found to drastically change from 5.9 ± 0.5 to 2.4 ± 0.2, ascribed to the release of phosphate ions into the media (Ahmed et al. 2004). A similar decrease was not observed for the samarium-containing microspheres. The changes in mass, size and pH media were also marginal as the microsphere products remained intact (see **Figure S2**, Supporting Information) until the end of the study at 28 days. Overall, the limited changes in the morphology, mass-loss, size and pH of media in the degradation study for the samarium containing microspheres suggested that they were highly stable and very durable.

The durability of radionuclide microspheres is an important aspect of internal radiotherapy, which can impact their chemical effectiveness and radionuclidic safety. In this study, high melt temperature samarium oxide (2,335 °C) was successfully incorporated into a phosphate-based glass (PBG) matrix and at remarkably high level (up to 44 ± 5 mol%). The relatively low-melt temperature characteristics of PBGs (as compared to silicate glasses) enabled the addition of high concentrations of samarium, which the authors have not seen achieved before. However, the impact of such incorporation led to the formation of glass-ceramic structure which

subsequently increased the durability of the microspheres formed, as confirmed by degradation analysis. This robustness was similarly observed in yttrium-doped aluminosilicate glass microspheres, where degradation studies showed low dissolution rates and minimal yttrium weight percentage (0.09 % Y released/gram) in 37 °C, DI H<sub>2</sub>O during the study (Erbe and Day 1993) underlining the high chemical durability of these microspheres.

Analysis of the radioactivity for the microspheres produced was conducted through neutron activation analysis using a medium thermal neutron flux  $3.01 \times 10^{13} \text{ n.cm}^{-2}.\text{s}^{-1}$  for only 15 minutes of irradiation time. The reaction occurred with  $^{152}\text{Sm}(n,\gamma)^{153}\text{Sm}$ , where samarium-152 atoms absorbed one neutron from the neutron flux, becoming radioactive samarium-153, where extra energy was also released as gamma radiation (Hashikin et al. 2015; Tan et al. 2022). The estimated radioactivity of samarium-153, specifically at  $103.1 \pm 0.2 \text{ keV}$ , was determined through gamma spectroscopy. As presented in **Table 3**, each sample's radioactivity was lower than 3 GBq/g (the dose currently available in yttrium-90 microspheres). An increase in irradiation time is known to be proportionally related to the increasing desired radioactivity of the sample (Tan et al., 2022). As such, further estimations of the samarium radioactivity were determined using the neutron activation formula [see **Equation 2**] in the result section. The obtained radioactivity value (**Table 3**) after 15 min of irradiation was used to determine the number of parent atoms (N) that were neutron-activated in each formulation. Thus, the irradiation time corresponding to 3 GBq/g activity can be determined.

The estimated activities calculated are shown in **Table 4**, where G50:Sm50 and G25:Sm75 achieved 3.23 and 3.47 GBq/g, respectively, needing only 90 minutes of irradiation time. For the lower samarium containing sample G75:Sm25, a dose of 3 GBq/g could be obtained if the sample was irradiated for 3 hours. It was also shown that the required irradiation time for each sample was relatively shorter (see **Table 5**) than the time suggested by Hashikin *et al.* (2015) and Wong *et al.* (2019) when they produced samarium microspheres. Hashikin *et al.* (2015) used commercially available Amberlite® IR-120 resin to prepare samarium-doped microparticles through an ion-exchange reaction method and obtained irregular-shaped particles resulting in their fragmentation during the neutron activation process. The activity of 3 GBq/g was achieved through 6 hours of neutron bombardment with thermal flux  $1.494 \times 10^{12} \text{ n.cm}^{-2}.\text{s}^{-1}$ . Furthermore, Wong *et al.* (2019) used the same ion-exchange resin method by doping  $\text{SmCl}_3/\text{Sm}_2(\text{CO}_3)_3$  with Toyopearl® microspheres, and they recommended that to achieve 5 GBq/g activity, the microspheres produced would need to be activated for 6 hours of

irradiation time. In comparison, if all three of the samarium microsphere sample ratios produced in this study were activated for 6 hours, their estimated activity would be 3 – 6 times higher than the activities of the yttrium-microspheres (TheraSphere™) currently available. Therefore, the samarium-doped phosphate microsphere samples produced in this study offer several potential benefits. For example, reducing the number of microspheres required for SIRT would also reduce the risk of increasing damage to normal liver tissue due to the possibility of particle reflux (Zhou et al., 2023). As such, the microspheres produced in this study would allow for the customisation of doses and particle quantity before administration. However, further studies are needed to determine the radioactivity equivalent between <sup>153</sup>Sm and 3 GBq.g<sup>-1</sup> of <sup>90</sup>Y since both radioisotopes have different beta emission energies.

**Table 5.** Radionuclide microspheres formulation study for internal radiation delivery

Properties	TheraSphere™ (Boston Scientific Corporation, Canada)	SIR-Spheres® (SIRTex, Sydney, Australia)	Sm-Amber (Hashikin, et al. 2015.PLoS One 10 (9))	Sm-PLLA (Wong et al. 2019. Pharmaceuticals 11 (11))	Samarium-doped phosphate glass microspheres (this study)
<b>Morphology</b>	Microspheres	Microspheres	Irregular microparticles	Microspheres	Microspheres
<b>Radionuclide/emitter</b>	<sup>90</sup> Y/ therapeutic β	<sup>90</sup> Y/ therapeutic β	<sup>153</sup> Sm/ therapeutic β and diagnostic γ	<sup>153</sup> Sm/ therapeutic β and diagnostic γ	<sup>153</sup> Sm/ therapeutic β and diagnostic γ
<b>T1/2 (h)</b>	64.08	64.08	46.32	46.32	46.32
<b>Matrix</b>	Glass	Resin	Resin-based (Amberlite™)	Acrylic-based (Toyopearl®)	Glass
<b>Radioactivity (GBq/g)</b>	3 – 20 (depend on the packaging dosage)	3	3.1 (6 hours irradiation time)	2.53 (6 hours irradiation time)	3.23 (G75:Sm25) 6.39 (G50:Sm50) 6.85 (G25:Sm75) - 3 hours irradiation time)

Overall, this study demonstrated that production of significantly high samarium content containing microspheres (i.e. up to 44% in G25:Sm75) could be achieved through flame spheroidisation with initial radioactivity analyses showing that therapeutic radiation doses could be achieved with less than 3 hours of sample irradiation. The samarium-doped microspheres were shown to be highly stable phosphate-glass ceramics. In this study, it is also

worth noting that we developed a simple and economical approach to incorporate stable radionuclide (non-radioactive) [ $^{152}\text{Sm}$ ] samarium oxide into phosphate-based glass matrix through flame spheroidisation process. This synthesis process was achievable without involving hazardous chemicals, solvents or radiation exposure, which can involve complex procedures. In addition, the microspheres produced would also allow for pretreatment dosimetry planning due to the theranostic properties owing to the use of  $^{153}\text{Sm}$ . This would efficiently shorten the treatment planning practice (as  $^{99\text{m}}\text{Tc}$ -macroaggregates albumin is used for scouting doses) before applying the  $^{90}\text{Y}$  (as pure  $\beta$  radiation) for internal radiotherapy applications. The samarium-containing microspheres produced would also provide non-complex post-treatment monitoring without using another radioactive microsphere like  $^{99\text{m}}\text{Tc}$ -MAA for distribution analysis due to  $\gamma$ -radiation, which is detectable through computed tomography, SPECT and MRI.

## 5. Conclusion

This study showed that samarium-doped phosphate glass microspheres were successfully developed into three different formulations, namely G75:Sm25, G50:Sm50 and G25:Sm75, through a flame spheroidization process, with uniform spherical shapes and high distribution of samarium content. The addition of samarium oxide to P60 glass resulted in microspheres with distinctive stability characteristics, which are desirable in formulating radionuclide microspheres to prevent radioactive leaking during internal radiotherapy. The samarium-doped phosphate glass microspheres formed a glass-ceramic structure that was not easily degraded and was stable for up to 28 days in Milli-Q water at  $37^\circ\text{C}$ . After 15 minutes of neutron activation in thermal neutron,  $3.01 \times 10^{13} \text{ n.cm}^{-2}.\text{s}^{-1}$ , the radioactivity of activated  $^{153}\text{Sm}$  was 0.58 GBq/g in G25:Sm75 with the estimation to be increased into 6.85 GBq/g with 3 hours irradiation time. This suggests that the formulations could be modified to achieve the required specific activity before internal radiation treatment. Importantly, these samarium microspheres are both beta emitters (for therapeutic) and gamma emitters (for diagnostic), which will avoid the need for complex pre-and post-treatment currently required for pure beta emitter radionuclide doped microspheres. Further studies, especially cytotoxicity and theranostic application, are required to enhance the properties of the microspheres with potential use as selective internal radiotherapy treatment applications.

## Acknowledgement

The authors would like to acknowledge the Indonesia Endowment Fund for Education (LPDP) for supporting this work through a Doctoral Grant awarded to Andi Arjuna (01688/MAT/D/BUDI-2019). The authors would also like to thank the Nanoscale and Microscale Research Centre (nmRC) at the University of Nottingham for the use of the electron microscope facilities, as well National Research and Innovation Agency - Indonesia (BRIN) and Universitas Hasanuddin - Indonesia for their support and help with this work.

## References

- Ahmed, I, M Lewis, I Olsen, and J C Knowles. 2004. "Phosphate Glasses for Tissue Engineering: Part 1. Processing and Characterisation of a Ternary-Based P2O5–CaO–Na2O Glass System." *Biomaterials* 25 (3): 491–99.
- Ahmed, Ifty, Hong Ren, and Jonathan Booth. 2019. "Developing Unique Geometries of Phosphate-Based Glasses and Their Prospective Biomedical Applications." *Johnson Matthey Technology Review* 63 (1): 34–42.  
<https://doi.org/10.1595/205651319X15426460058863>.
- Anderson, Pete, and Rodolfo Nunez. 2007. "Samarium Lexidronam (153Sm-EDTMP): Skeletal Radiation for Osteoblastic Bone Metastases and Osteosarcoma." *Expert Review of Anticancer Therapy* 7 (11): 1517–27.
- Arafat, Abul, Sabrin A Samad, Jeremy J Titman, Andrew L Lewis, Emma R Barney, and Ifty Ahmed. 2020. "Yttrium Doped Phosphate-Based Glasses: Structural and Degradation Analyses." *Biomedical Glasses* 6 (1): 34–49.
- Arafat, Abul, Sabrin A Samad, Matthew D Wadge, Md Towhidul Islam, Andrew L Lewis, Emma R Barney, and Ifty Ahmed. 2020. "Thermal and Crystallization Kinetics of Yttrium- doped Phosphate- based Glasses." *International Journal of Applied Glass Science* 11 (1): 120–33.
- Bruix, Jordi, Maria Reig, and Morris Sherman. 2016. "Evidence-Based Diagnosis, Staging, and Treatment of Patients with Hepatocellular Carcinoma." *Gastroenterology* 150 (4): 835–53.
- d'Abadie, Philippe, Michel Hesse, Amandine Louppe, Renaud Lhommel, Stephan Walrand, and Francois Jamar. 2021. "Microspheres Used in Liver Radioembolization: From Conception to Clinical Effects." *Molecules* 26 (13): 3966.
- Donanzam, B. A., T. P.R. Campos, I. Dalmázio, and E. S. Valente. 2013. "Synthesis and Characterisation of Calcium Phosphate Loaded with Ho-166 and Sm-153: A Novel Biomaterial for Treatment of Spine Metastases." *Journal of Materials Science: Materials in Medicine* 24 (12): 2873–80. <https://doi.org/10.1007/s10856-013-5024-0>.
- Dousti, M Reza, S K Ghoshal, Raja J Amjad, M R Sahar, Fakhra Nawaz, and R Arifin. 2013. "Structural and Optical Study of Samarium Doped Lead Zinc Phosphate Glasses." *Optics Communications* 300: 204–9.
- Erbe, Erik M, and Delbert E Day. 1993. "Chemical Durability of Y2O3- Al2O3- SiO2 Glasses for the in Vivo Delivery of Beta Radiation." *Journal of Biomedical Materials Research* 27 (10): 1301–8.



- Foglia, Beatrice, Cristian Turato, and Stefania Cannito. 2023. "Hepatocellular Carcinoma: Latest Research in Pathogenesis, Detection and Treatment." *International Journal of Molecular Sciences*. MDPI.
- Hashikin, N A A, C H Yeong, B J J Abdullah, K H Ng, L Y Chung, R Dahalan, and A C Perkins. 2015. "Samarium-153 Labelled Microparticles for Targeted Radionuclide Therapy of Liver Tumor." In *World Congress on Medical Physics and Biomedical Engineering, June 7-12, 2015, Toronto, Canada*, 471–74. Springer.
- Hashikin, Nurul Ab Aziz, Chai-Hong Yeong, Basri Johan Jeet Abdullah, Kwan-Hoong Ng, Lip-Yong Chung, Rehir Dahalan, and Alan Christopher Perkins. 2015. "Neutron Activated Samarium-153 Microparticles for Transarterial Radioembolization of Liver Tumour with Post-Procedure Imaging Capabilities." *PLoS One* 10 (9): e0138106.
- Hossain, Kazi M.Zakir, Uresha Patel, Andrew R. Kennedy, Laura Macri-Pellizzeri, Virginie Sottile, David M. Grant, Brigitte E. Scammell, and Ifty Ahmed. 2018. "Porous Calcium Phosphate Glass Microspheres for Orthobiologic Applications." *Acta Biomaterialia* 72: 396–406. <https://doi.org/10.1016/j.actbio.2018.03.040>.
- Hussain, Saddam, Raja J Amjad, Muhammad Tanveer, Muhammad Nadeem, Hasan Mahmood, Abdul Sattar, Azmat Iqbal, Irshad Hussain, Z Amjad, and Syed Zajif Hussain. 2017. "Optical Investigation of Sm 3+ Doped in Phosphate Glass." *Glass Physics and Chemistry* 43: 538–47.
- Islam, Md Towhidul, Reda M. Felfel, Ensanya A. Abou Neel, David M. Grant, Ifty Ahmed, and Kazi M.Zakir Hossain. 2017. "Bioactive Calcium Phosphate-Based Glasses and Ceramics and Their Biomedical Applications: A Review." *Journal of Tissue Engineering* 8. <https://doi.org/10.1177/2041731417719170>.
- Kao, Yung-Hsiang, Jeffrey D Steinberg, Young-Soon Tay, Gabriel K Y Lim, Jianhua Yan, David W Townsend, Angela Takano, Mark C Burgmans, Farah G Irani, and Terence K B Teo. 2013. "Post-Radioembolization Yttrium-90 PET/CT-Part 1: Diagnostic Reporting." *EJNMMI Research* 3: 1–13.
- Kauffman, Nathan, James Morrison, Kevin O'Brien, Jinda Fan, and Kurt R Zinn. 2023. "Intra-Arterial Delivery of Radiopharmaceuticals in Oncology: Current Trends and the Future of Alpha-Particle Therapeutics." *Pharmaceutics* 15 (4): 1138.
- Kaur, Jaspreet, Paramvir Kaur, Isha Mudahar, and K Singh. 2023. "Effect of Sm<sub>2</sub>O<sub>3</sub> on the Physical, Structural and Optical Properties of 40 SiO<sub>2</sub>-40 B<sub>2</sub>O<sub>3</sub>-10 V<sub>2</sub>O<sub>5</sub>-(10-x) Fe<sub>2</sub>O<sub>3</sub> Glasses." *Ceramics International* 49 (9): 13610–17.
- Kawashita, Masakazu, Naoko Matsui, Zhixia Li, Toshiki Miyazaki, and Hiroyasu Kanetaka. 2011. "Preparation, Structure, and in Vitro Chemical Durability of Yttrium Phosphate Microspheres for Intra- arterial Radiotherapy." *Journal of Biomedical Materials Research Part B: Applied Biomaterials* 99 (1): 45–50.
- Knapp, Furn F, and Ashutosh Dash. 2016. *Radiopharmaceuticals for Therapy*. Springer.
- Lim, Hyun-Ji, Min-Seung Kang, Imjeong H S Yang, Mirang Byeon, Hyun Gyu Kim, Jong Seong Bae, and Kyong-Soo Hong. 2021. "Structures and Photophysical Characterisation of the Samarium-Doped Y<sub>2</sub>Mo<sub>3</sub>O<sub>12</sub> Ceramics."
- "Liver Cancer Statistics | Cancer Research UK." n.d. Accessed March 24, 2023. <https://www.cancerresearchuk.org/health-professional/cancer-statistics/statistics-by->

- cancer-type/liver-cancer#heading-Two.
- Marzouk, M A, H A ElBatal, Y M Hamdy, and F M Ezz-Eldin. 2019. "Collective Optical, FTIR, and Photoluminescence Spectra of CeO<sub>2</sub> and/or Sm<sub>2</sub>O<sub>3</sub>-Doped Na<sub>2</sub>O–ZnO–P<sub>2</sub>O<sub>5</sub> Glasses." *International Journal of Optics* 2019.
- Meza-Junco, Judith, Aldo J Montano-Loza, David M Liu, Michael B Sawyer, Vincent G Bain, Mang Ma, and Richard Owen. 2012. "Locoregional Radiological Treatment for Hepatocellular Carcinoma; Which, When and How?" *Cancer Treatment Reviews* 38 (1): 54–62.
- Milborne, Ben, Abul Arafat, Rob Layfield, Alexander Thompson, and Ifty Ahmed. 2020. "The Use of Biomaterials in Internal Radiation Therapy." *Recent Progress in Materials* 2 (2).
- Milborne, Ben, Lauren Murrell, Ian Cardillo-Zallo, Jeremy Titman, Louise Briggs, Colin Scotchford, Alexander Thompson, Robert Layfield, and Ifty Ahmed. 2022. "Developing Porous Ortho-and Pyrophosphate-Containing Glass Microspheres; Structural and Cytocompatibility Characterisation." *Bioengineering* 9 (11): 611.
- Molinar Díaz, Jesús, Sabrin Abdus Samad, Elisabeth Steer, Nigel Neate, Hannah Constantin, Md Towhidul Islam, Paul D Brown, and Ifty Ahmed. n.d. "Flame Spheroidisation of Dense and Porous Ca<sub>2</sub>Fe<sub>2</sub>O<sub>5</sub> Microspheres." *Materials Advances*.
- Nijssen, J F W, B A Zonnenberg, J R W Woittiez, D W Rook, I A Swildens-van Woudenberg, P P Van Rijk, and A D Van het Schip. 1999. "Holmium-166 Poly Lactic Acid Microspheres Applicable for Intra-Arterial Radionuclide Therapy of Hepatic Malignancies: Effects of Preparation and Neutron Activation Techniques." *European Journal of Nuclear Medicine* 26: 699–704.
- Pasciak, Alexander S, Austin C Bourgeois, J Mark McKinney, Ted T Chang, Dustin R Osborne, Shelley N Acuff, and Yong C Bradley. 2014. "Radioembolisation and the Dynamic Role of 90Y PET/CT." *Frontiers in Oncology* 4: 38.
- Peltek, Oleksii O., Albert R. Muslimov, Mikhail V. Zyuzin, and Alexander S. Timin. 2019. "Current Outlook on Radionuclide Delivery Systems: From Design Consideration to Translation into Clinics." *Journal of Nanobiotechnology* 17 (1): 1–34. <https://doi.org/10.1186/s12951-019-0524-9>.
- Sadler, Alexander W E, Leena Hogan, Benjamin Fraser, and Louis M Rendina. 2022. "Cutting Edge Rare Earth Radiometals: Prospects for Cancer Theranostics." *EJNMMI Radiopharmacy and Chemistry* 7 (1): 1–55.
- Sharifi, Esmaeel, Ashkan Bigham, Satar Yousefiasl, Maria Trovato, Matineh Ghomi, Yasaman Esmaeili, Pouria Samadi, Ali Zarrabi, Milad Ashrafizadeh, and Shokrollah Sharifi. 2022. "Mesoporous Bioactive Glasses in Cancer Diagnosis and Therapy: Stimuli- responsive, Toxicity, Immunogenicity, and Clinical Translation." *Advanced Science* 9 (2): 2102678.
- Sofou, Stavroula. 2008. "Radionuclide Carriers for Targeting of Cancer." *International Journal of Nanomedicine* 3 (2): 181–99.
- Tan, Hun Yee, Yin How Wong, Azahari Kasbollah, Mohammad Nazri Md Shah, Basri Johan Jeet Abdullah, Alan Christopher Perkins, and Chai Hong Yeong. 2022. "Development of Neutron-Activated Samarium-153-Loaded Polystyrene Microspheres as a Potential

- Theranostic Agent for Hepatic Radioembolization.” *Nuclear Medicine Communications* 43 (4): 410–22.
- Valente, Eduardo Sarmento, Ethel Mizrahy Cuperschmid, and Tarcísio Passos Ribeiro de Campos. 2011. “Characterisation of Ceramic Seeds with Samarium-153 for Use in Brachytherapy.” *Materials Research* 14 (1): 21–24.
- Weber, Manuel, M Lam, Carlo Chiesa, Mark Konijnenberg, Marta Cremonesi, Patrick Flamen, Silvano Gnesin, Lisa Bodei, T Kracmerova, and Markus Luster. 2022. “EANM Procedure Guideline for the Treatment of Liver Cancer and Liver Metastases with Intra-Arterial Radioactive Compounds.” *European Journal of Nuclear Medicine and Molecular Imaging* 49 (5): 1682–99.
- Wong, Yin-How, Hun-Yee Tan, Azahari Kasbollah, Basri Johan Jeet Abdullah, Rajendra Udyavara Acharya, and Chai-Hong Yeong. 2020. “Neutron-Activated Biodegradable Samarium-153 Acetylacetonate-Poly-L-Lactic Acid Microspheres for Intraarterial Radioembolization of Hepatic Tumors.” *World Journal of Experimental Medicine* 10 (2): 10.
- Wong, Yin How, Hun Yee Tan, Azahari Kasbollah, Basri Johan Jeet Abdullah, and Chai Hong Yeong. 2019. “Preparation and in Vitro Evaluation of Neutron-Activated, Theranostic Samarium-153-Labeled Microspheres for Transarterial Radioembolization of Hepatocellular Carcinoma and Liver Metastasis.” *Pharmaceutics* 11 (11). <https://doi.org/10.3390/pharmaceutics11110596>.
- Yeong, Chai Hong, Yin Wong, Hun Yee Tan, Azahari Kasbollah, and Basri Johan Jeet Abdullah. 2020. “Production of Theranostic 153 Samarium-Labelled Polystyrene Microparticles for Hepatic Radioembolization.” In *Trends in Radiopharmaceuticals (ISTR-2019). Proceedings of an International Symposium. Programme and Abstracts*.
- Zhou, Yi, Yun Gao, Guangxin Duan, Ling Wen, Shanshan Shan, Shuwang Wu, Jianfeng Zeng, and Mingyuan Gao. 2023. “Radioactive Microspheres for Selective Internal Radiation Therapy of Hepatocellular Carcinoma.” *Advanced NanoBiomed Research*, 2200166.

Ms. Ref. No.: IJPHARM-D-23-03505

Title: Development of samarium doped phosphate glass microspheres for internal radiotherapy applications

### Response to reviewers

We are very thankful to the reviewers for taking the time to review and provide helpful comments to improve our manuscript. We have addressed each reviewer's comments in detail, please see below (*the reviewer's comments are highlighted in italics and our response is in blue*).

#### Reviewer#1

*The manuscript under discussion reports development of the appropriately loaded uniform spherical samarium-doped phosphate glass microspheres through flame spheroidization process. The resultant microspheres were stable and radioactivity-leakage free during possible internal radiotherapy. The required specific activity was possible to be achieved by controlling certain factors before internal radiation treatment and the microspheres, being constituting samarium, emits both, the beta and gamma emitter could be used for theranostic purpose without the requirements of the complex pre- and post- treatments, as needed for the currently used pure beta emitter yttrium-90. There are few suggestions and comments for enhancing the manuscript.*

- 1. The authors are required to read the manuscript carefully for spelling and grammatical errors.*
- 2. Please avoid use the personalised words such as we, our, etc in the manuscript.*

#### Response to reviewer

We thank the reviewer for this suggestion. We have reviewed and corrected the spelling and grammar in the manuscript as requested. Further, we have also updated the manuscript to avoid the use of personalised words.

- 3. Since samarium is beta as well as gamma emitter, the title should reflect this aspect and the title of the manuscript may be "Development of samarium doped phosphate glass microspheres for internal radiotheranostic applications".*

#### Response to reviewer

We thank the reviewer for this suggestion and have updated our manuscript title to "Development of samarium-doped phosphate glass microspheres for internal radiotheranostic applications".

- 4. Rephrase the sentence in Line 16.*

#### Response to reviewer

As suggested by the reviewer, the L16 sentence was rephrased and amended in the abstract as follows:

L16\_ Internal radiotherapy delivers radioactive sources inside the body, near to or into malignant tumours, which may be particularly effective when malignancies are not responding to external beam radiotherapy.

5. *First spell the word in full before use of the abbreviations/symbols.*

#### Response to reviewer

As suggested by the reviewer, the following abbreviation details were amended in the abstract.

L23\_...Scanning electron microscopy (SEM) and Energy dispersive X-ray (EDX)

L26\_...X-Ray diffraction (XRD)

6. *It is opined that the affirmative sentences, such as "...Therefore, this study confirms that..." should be avoided.*

#### Response to reviewer

As suggested by the reviewer, the following L31 sentence was amended in the abstract.

L31\_ "Therefore, the samarium microspheres produced in this study"....

7. *There is a need to be specify the cancer types, i.e., hepatic and bone cancers that could possibly be treated with the developed microspheres.*

#### Response to reviewer

As suggested by the reviewer, the following sentence to specify the type of cancer was added to the abstract.

L32\_ "..... provide great potential for improving internal radiotherapy treatment for liver cancer by ....".

8. *Under the heading of statistics, remove "all" from the sentence "When it is applicable, all the data....*

#### Response to reviewer

As suggested by the reviewer, the following L219 were amended in the materials and methods section.

L219\_ "All data were presented, calculated and processed using GraphPad Prism. Where it is applicable, the data displayed is based on mean  $\pm$  SD".

9. *Comment, briefly about the possible biodegradation of microspheres and on the chemical and radio nuclidic purity, which may be supported through literature.*

#### Response to reviewer

As suggested, we have added the following details to the discussion section:

"The durability of radionuclide microspheres is an important aspect of internal radiotherapy, which can impact their chemical effectiveness and radionuclidic safety. In this study, high melt

temperature samarium oxide (2,335 °C) was successfully incorporated into a phosphate-based glass (PBG) matrix and at remarkably high level (up to  $44 \pm 5$  mol%). The relatively low-melt temperature characteristics of PBGs (as compared to silicate glasses) enabled the addition of high concentrations of samarium, which the authors have not seen achieved before. However, the impact of such incorporation led to the formation of glass-ceramic structure which subsequently increased the durability of the microspheres formed, as confirmed by degradation analysis. This robustness was similarly observed in yttrium-doped aluminosilicate glass microspheres, where degradation studies showed low dissolution rates and minimal yttrium weight percentage (0.09 % Y released/gram) in 37 °C, DI H<sub>2</sub>O during the study (Erbe and Day 1993), underlining the high chemical durability of these microspheres”.

10. *Optionally consolidate the information on the limitations of <sup>90</sup>Y microspheres and others conventional therapies and the possible advantages of the currently developed samarium microspheres as a table.*

#### Response to reviewer#10

We thank the reviewer for this insightful suggestion. Indeed, we have outlined the limitations of <sup>90</sup>Y microspheres in the introduction sections (L58-68), highlighting that the samarium microspheres developed in this study aimed to address these limitations. Furthermore, we have explained the advantages of producing samarium microspheres over yttrium in the discussion sections (L456-463 and L476-483). Additionally, in L446-455 we compared the recently developed samarium-doped phosphate glass microspheres radioactivity with previous samarium-based polymer microparticles prepared by Hashikin et al. (2015) and Wong et al. (2019). This information is also provided as a Table 5 in the discussion section.

*Table 5. Radionuclide microspheres formulation study for internal radiation delivery*

Properties	<b>TheraSphere<sup>TM</sup></b> (Boston Scientific Corporation, Canada)	<b>SIR-Spheres<sup>®</sup></b> (SIRTex, Sydney, Australia)	<b>Sm-Amber</b> (Hashikin, et al. 2015.PLoS One 10 (9))	<b>Sm-PLLA</b> (Wong et al. 2019. Pharmaceutics 11 (11))	<b>Samarium-doped phosphate glass microspheres (this study)</b>
<b>Morphology</b>	Microspheres	Microspheres	Irregular microparticles	Microspheres	Microspheres
<b>Radionuclide/emitter</b>	<sup>90</sup> Y/ therapeutic β	<sup>90</sup> Y/ therapeutic β	<sup>153</sup> Sm/ therapeutic β and diagnostic γ	<sup>153</sup> Sm/ therapeutic β and diagnostic γ	<sup>153</sup> Sm/ therapeutic β and diagnostic γ
<b>T1/2 (h)</b>	64.08	64.08	46.32	46.32	46.32
<b>Matrix</b>	Glass	Resin	Resin-based (Amberlite <sup>TM</sup> )	Acrylic-based (Toyopearl <sup>®</sup> )	Glass
<b>Radioactivity (GBq/g)</b>	3 – 20 (depend on the packaging dosage)	3	3.1 (6 hours irradiation time)	2.53 (6 hours irradiation time)	3.23 (G75:Sm25) 6.39 (G50:Sm50) 6.85 (G25:Sm75) - 3 hours irradiation time)

11. *The major advantage of the samarium-doped phosphate glass microspheres is that they could be prepared using a cold (non-radioactive) procedure. This fact is required to be highlighted more in the Discussion Section.*

Response to reviewer

We have added the following details to the discussion section based on the comments above.

L478-L483: "In this study it is also worth noting that we developed a simple and economical approach to incorporate stable (non-radioactive) radionuclide [<sup>152</sup>Sm] samarium oxide into phosphate-based glass matrix through the flame spheroidisation process. This synthesis process was achievable without involving hazardous chemicals, solvents or radiation exposure, which can involve complex procedures".

12. *Remove "treatment" from the phrase "internal radiotherapy treatment".*

Response to reviewer

As suggested, we have updated the conclusion section accordingly.

13. *The Figure 5C is without description of the studied microsphere types.*

Response to reviewer

As suggested, we have updated the caption for Figure 5C and its description.

Reviewer#2

*The manuscript is well written, several comments to improve the quality of the manuscript:*

1. *Please check the typo throughout the manuscript.*

Response to reviewer

Following the suggestion from both reviewers, we have reviewed and corrected the spelling and grammar in our manuscript.

2. *Why did the authors perform the study (Section 2.8) in water instead of buffer with physiological condition?*

Response to reviewer

This is an excellent question from the reviewer and we acknowledge that using a buffer such as phosphate buffered solution (PBS) would also be a good choice of media. In this study, MilliQ-water was used as media for the general degradation study, for the following reasons. 1) MilliQ-water has high purity and low ionic content, which minimises potential interference during the initial study, and also provides a controlled environment for studying the degradation profile and products from the glass microspheres (Hossain et al. 2018) 2) MilliQ water is much harsher and has stronger degradation attack than PBS or other media, as the ions in those media can actually inhibit degradation mechanisms.

3. *Please explain the statistical method used in Section 2.11?*

#### Response to reviewer

We applied simple statistical analysis by calculating and presenting data as the average and standard deviation from the minimal three data points collected. We have also updated the statistical section in the materials and methods section to highlight this.

4. *In Figure 1, the surface of the particles from different formulation was different. Could the author explain this?*

#### Response to reviewer

We are pleased that the reviewer noted this and acknowledged that there was a noticeable change in microsphere surface features, especially with increasing samarium content. Starting from the P60 control microspheres, all microspheres appeared to have a smooth surface. However, with increasing concentrations of samarium oxide, distinguishable topographical features became visible on the microspheres surface. As described from the SEM and EDX mapping, we defined these features as samarium crystallisation, which was also in line with the results from XRD analysis which showed that the samarium-doped microspheres produced formed glass-ceramic structures. These topographical features are still under exploration and will feature as a follow-up study and publication.

#### Comments from the editor

*Figures 3 and 4: please add the y-axis to the figures*

#### Response to editor

As suggested, we have also updated Figures 3 and 4.

#### **References**

- Erbe, Erik M, and Delbert E Day. 1993. "Chemical Durability of Y<sub>2</sub>O<sub>3</sub>-Al<sub>2</sub>O<sub>3</sub>-SiO<sub>2</sub> Glasses for the in Vivo Delivery of Beta Radiation." *Journal of Biomedical Materials Research* 27 (10): 1301–8.
- Hashikin, Nurul Ab Aziz, Chai-Hong Yeong, Basri Johan Jeet Abdullah, Kwan-Hoong Ng, Lip-Yong Chung, Rehir Dahalan, and Alan Christopher Perkins. 2015. "Neutron Activated Samarium-153 Microparticles for Transarterial Radioembolization of Liver Tumour with Post-Procedure Imaging Capabilities." *PLoS One* 10 (9): e0138106.
- Hossain, Kazi M.Zakir, Uresha Patel, Andrew R. Kennedy, Laura Macri-Pellizzeri, Virginie Sottile, David M. Grant, Brigitte E. Scammell, and Ifty Ahmed. 2018. "Porous Calcium Phosphate Glass Microspheres for Orthobiologic Applications." *Acta Biomaterialia* 72: 396–406. <https://doi.org/10.1016/j.actbio.2018.03.040>.
- Wong, Yin How, Hun Yee Tan, Azahari Kasbollah, Basri Johan Jeet Abdullah, and Chai Hong Yeong. 2019. "Preparation and in Vitro Evaluation of Neutron-Activated, Theranostic Samarium-153-Labeled Microspheres for Transarterial Radioembolization of Hepatocellular Carcinoma and Liver Metastasis." *Pharmaceutics* 11 (11). <https://doi.org/10.3390/pharmaceutics11110596>.



